

低碳钢双丝焊平板横向残余应力超声波法测量

路 浩¹, 刘雪松¹, 杨建国¹, 张世平², 方洪渊¹

(1. 哈尔滨工业大学 现代焊接生产技术国家重点实验室, 哈尔滨 150001;
2. 哈尔滨工业大学 电气工程学院, 哈尔滨 150001)



路 浩

摘 要: 介绍了超声波法应力测量的理论基础声弹性方程, 特殊条件下简化临界折射纵波声弹性方程。建立了超声波法测量焊接残余应力系统, 实现了高精度信号提取, 使用特制变角度超声波探头, 选用对应力变化敏感的临界折射纵波作为测量波形, 对低碳钢双丝焊对接平板横向残余应力场实现了无损测量。结果表明, 测量结果可靠, 测量过程实时无损快速。分析了测量数据波动的原因。建立的超声波法应力无损测量系统为焊接结构服役状态在线可靠性评估奠定了基础。

关键词: 超声波法; 横向残余应力; 临界折射纵波

中图分类号: TG404 **文献标识码:** A **文章编号:** 0253—360X(2008)05—0030—03

0 序 言

在结构服役状态下无损测量其内部残余应力分布, 对焊接结构可靠性评估具有重要意义。目前应用的残余应力测量方法局限性很大, 例如小孔法准确但对工件造成破坏, X 射线衍射法测量深度低等, 而且这些方法操作复杂, 费时耗力。超声波法测量应力以声弹性学理论为理论基础, 可以无损快速实时地检测出残余应力。

文中介绍了超声波法测量焊接残余应力研究最新进展。建立的超声波法残余应力测量系统, 实现了高精度的信号采集, 使用特制变角度超声波斜探头产生了临界折射纵波, 标定了低碳钢临界折射纵波声弹性常数, 对低碳钢平板双丝焊横向残余应力场进行了无损测量, 并分析了数据波动的原因。

1 声弹性方程

1953 年 Hughes 等人^[1-6] 导出了声弹性方程早期表达形式, 描述了材料中声波传播速度与应力之间的关系, 奠定了声弹性理论基础。此后多人不断对理论进行完善。

声弹性方程推导有以下假设: 物体连续性, 物体

是超弹性的、均匀的, 声波的小扰动叠加在物体的静态有限变形上, 变形过程等熵。

物体处于无应力、应变的状态为未变形状态, 称为状态 I; 物体在某一载荷作用下的状态为初始状态, 称为状态 II; 预变形的物体上叠加声波小扰动, 物体进一步变形达到的状态为最终状态, 即超声波检测状态, 称为状态 III。质点的位置用矢量 \mathbf{X} 表示, 相应的分量分别以希腊字母、大写罗马字母和小写罗马字母为下标。

初始坐标下应力介质中弹性波动方程为

$$\frac{\partial}{\partial \mathbf{X}_j} \left[\left(\delta_{jk} \dot{t}_{jL} + C_{IKL} \right) \frac{\partial u_K}{\partial \mathbf{X}_L} \right] = \rho^i \frac{\partial u_i}{\partial t^2} \tag{1}$$

式中: δ_{jk} 为 Kronecker delta 函数; u 是动态位移; C_{IKL} 为等效刚度, 取决于材料常数和初始位移场; ρ^i 为物体受力状态下密度; \dot{t}_{jL} 为初始坐标描述的物体受力状态下柯西应力。

各向同性、材料轴和应力轴同向条件下, 沿应力方向传播纵波的声弹性方程为

$$\rho_0 V_{III}^2 = \lambda + 2\mu + \frac{R}{3K_0} \left[2l + \lambda + \frac{\lambda + \mu}{\mu} (4m + 4\lambda + 10\mu) \right] \tag{2}$$

式中: V_{III} 为沿应力方向传播纵波; K_0 为体积弹性模量; l, m 为三阶弹性常数; λ, μ 为二阶弹性常数; ρ_0 表示初始密度; R 为应力。

更一般的表达式, 特别对临界折射纵波(L_{cr})为

$$R = \frac{1}{K_i} \left[\frac{t_0 - t}{t_0} \right] \tag{3}$$

收稿日期: 2007—06—27
基金项目: 黑龙江省博士后资助项目 (FFCZ98505364); 中俄政府间科技合作项目 (2007DFR70070)

式中: t_0 , t 为无应力状态和应力状态下声波的传播时间; K_i 为声弹性常数。

2 超声波法焊接残余应力实时测量系统

设计建立的超声波法测量焊接残余应力系统, 如图 1 所示。硬件系统包括汕头超声所 CTS — 22 型超声波发生仪, 自制特殊可变角度探头, 带有特殊数据采集卡的 Tektronix 示波器。实时测量系统支持软件由虚拟仪器软件 Labview 编写。搭建的试验系统实现了纳秒精度的信号采集, 满足超声波法应力测量需要的精度。试验系统的特点是可以实时快速地进行焊接残余应力的测量, 每测量点单次测量时间不超过 10 s。工件由两块长 320 mm, 宽 200 mm, 厚 12 mmV 形坡口的平板对焊而成, 焊接工艺参数见表 1。

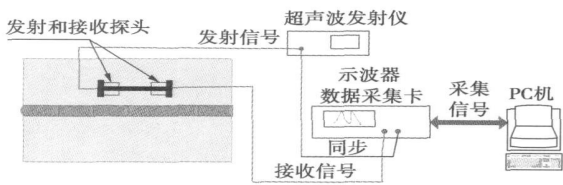


图 1 试验系统图
Fig 1 Schematic diagram of experimental setup

表 1 低碳钢平板双丝焊工艺参数
Table 1 Welding parameters

前丝电流	后丝电流	前丝电压	后丝电压	焊枪速度	送气量
I_1/A	I_2/A	U_1/V	U_2/V	$v/(\text{mm}\cdot\text{s}^{-1})$	$q/(\text{L}\cdot\text{min}^{-1})$
250	290	30	27.8	7	15

3 波形选择及弹性常数标定

文中使用特制可变角度探头产生临界折射纵波, 对工件焊接残余应力进行测量。其传播范围在工件临近表面下, 具有一定深度, 传播深度与其波长有关。声弹性常数表征弹性波声波的传播速度与应力之间的关系。弹性常数的精确确定是超声波法测量应力的基础, 其精确度决定了应力值的精度。在 INSTRON5500R 拉伸试验机上进行标定试验, 标定严格在恒定温度下进行, 标定试件长 9 mm, 宽 26 mm, 表面加工精度高, 避免毛刺带来的应力集中。临界折射纵波声弹性常数标定曲线如图 2 所示。根据试验数据拟合结果, 声弹性常数计算结果为 $1.458\times$

10^{-5} MPa^{-1} 。由声速波动引起的误差约为 $\pm 5\times 10^{-8} \text{ MPa}^{-1}$ 。

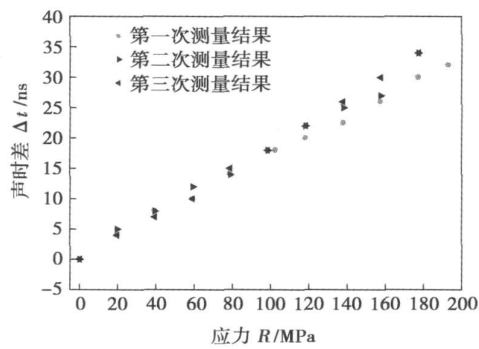


图 2 声弹性常数标定曲线
Fig 2 Acoustoelastic coefficient calibration curve

4 试验结果分析

试验在恒定温度下进行。测量前焊件表面用稀盐酸酸洗, 去除氧化层对探头移动的影响, 不破坏焊后应力状态。

首先测得应力引起的声时差, 根据声弹性常数换算为残余应力分布。得到的横向应力值测量结果如图 3 所示。探头中心距焊缝中心为 5 mm, 所测横向应力为距焊缝中心 75 mm, 且与焊缝平行的测量线上的应力分布。拉应力引起声波传播时间变长, 声速变慢, 压应力引起声波传播时间变短, 声速变快。测量深度约 2 mm, 由其波长决定。

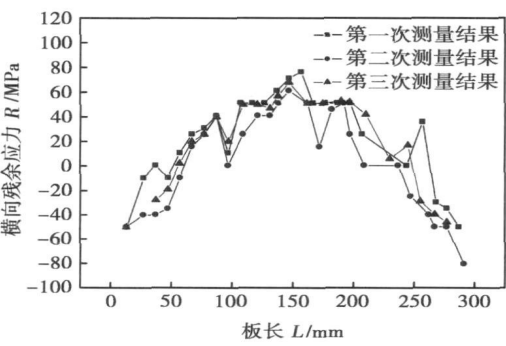


图 3 横向残余应力分布
Fig 3 Transverse residual stress distribution

造成数据波动的原因主要有以下几点。(1) 探头的夹持和移动方式精确性有待提高。(2) 声弹性方程在一系列假设基础上导出, 特别是没有考虑塑性过程。(3) 周围环境噪声对测量系统的影响。

5 结 论

- (1) 特殊探头产生的临界折射纵波对应力变化敏感。
- (2) 设计建立的超声波法测量焊接残余应力系统, 实现了平板焊接残余应力场的无损测量, 测量结果可靠, 测量过程快速、无损、实时, 测量系统完全可以应用到实际工程中。
- (3) 建立的超声波法应力无损测量系统为焊接结构服役状态在线可靠性评估奠定了基础。

参考文献:

[1] Hughes D S. Ultrasonic velocity in an elastic solid[J] . Journal of Applied Physics, 1950, 21(3): 294—301.

[2] Tokuoka T, Iwashimizu Y. A coustical birefringence of ultrasonic waves in deformed isotropic elastic materials[J] . International Journal of Solids Structures, 1968 4: 383—389.

[3] Fukuoka H, Toda H, Yamane T. A coustoelastic stress analysis of residual stress in a patch-welded disk[J] . Experimental Mechanics, 1978, 7: 277—280.

[4] Yabdallahoui H, Walaszek, Peyrac C, *et al.* The use of ultrasonic in the optimization of welding processes[J] . Welding International, 2001, 15(4): 1—12.

[5] Egle D M, Bray D E. Measurement of acoustoelastic and third—order elastic constants for rail steel[J] . The Journal of the Acoustical Society of America, 1976, 60(3): 741—744.

[6] Man C, Lu W Y. Towards an acoustoelastic theory for measurement of residual stress[J] . Journal of Elasticity, 1987 17: 159—182.

作者简介: 路 浩, 男, 1981 年出生, 博士研究生。主要研究方向为焊接结构可靠性评价及焊接结构残余应力无损测量。发表论文 6 篇。

Email: lhhit9@163.com

sidity to purify the weld metal. However, when the covering basicity is excessively high, the impact work at $-50\text{ }^{\circ}\text{C}$ can't increase any more; and the increase of the covering basicity makes against decreasing the diffusible hydrogen value in the deposited metal. So other methods have been applied to the electrode, such as dehydrating covering materials at quite high temperature, or repeatedly drying the electrode. Finally, all tests indicate that the deposited metal of the electrode can simultaneously have quite high yield strength, quite high impact work and quite low diffusible hydrogen value under optimizing process parameters.

Key words: high strength; impact work; diffusible hydrogen; covering basicity

Fretting wear behaviour of FeNiBSiCe alloy flame sprayed coatings LIANG Bunv¹, ZHANG Penlin², ZHANG Zhenyu^{1,2} (1. Mechanical Engineering Department, Lanzhou Polytechnic College, Lanzhou, 730050, China; 2. State Key Laboratory of New Nonferrous Metal Materials, Lanzhou University of Science & Technology, Lanzhou 730050, China). p21–24

Abstract The fretting wear properties of FeNiBSiCe alloy coatings coupling with SAE52100 steel under reciprocating sliding were examined by using a ball-on-disc reciprocating tribotester. Effects of load and sliding speed on fretting tribological properties of the coatings were studied. Worn surfaces of the coatings were analyzed by a scanning electron microscopy (SEM), a field emission scanning electron microscopy (FESEM) and energy dispersive spectroscopy (EDS), respectively. The friction coefficient of the coatings decreased slightly with the load, but increased with sliding speed at first, and then tended to be a constant value. The wear rate of the coatings increased with the load, but dramatically decreased at first and then slightly decreased with the sliding speed. An adhered oxide debris layer was formed on the worn surface in friction. Fretting wear mechanism of the coatings was microploUGH at normal load, microfracture, oxidation wear and a large amount of counterpart material was transferred to the coatings at high load and high sliding speed.

Key words: FeNiBSiCe coating; fretting wear; wear mechanism; fatigue delamination; oxide layer

Diffusion coefficient during diffusion bonding of surface self-nanocrystallization 0Cr18Ni9Ti and TA17 HAN Jing¹, SHENG Guangmin¹, HU Guoxiong¹, QIN Bin² (1. College of Materials Science & Engineering, Chongqing University, Chongqing 400030, China; 2. Research Institute for Stainless Steel Baosteel R & D Centre, Shanghai 200431, China). p25–29

Abstract The surface self-nanocrystallization was applied to ends of 0Cr18Ni9Ti stainless steel and TA17 near α titanium alloy bars by means of high energy shot peening (HESP), nanostructured surface layers on the ends of samples were obtained. Pulse-pressure diffusion bonding (PPDB) of 0Cr18Ni9Ti stainless steel and TA17 titanium alloy with nanostructured layers was carried out at $825\text{ }^{\circ}\text{C}$ within 180 s. Tighten diffusion bonding joint of 0Cr18Ni9Ti and TA17 which tensile strength is 221.6 MPa were formed. And the atomic diffusion concentrations near interface were measured by using energy spectrometer. The diffusion coefficient of Fe atom during dif-

fusion bonding in TA17 titanium alloy was achieved, the result shows that the diffusion coefficient of atoms during short-time diffusion bonding can be enhanced after 0Cr18Ni9Ti stainless steel and TA17 near α titanium alloy were treated.

Key words: surface self-nanocrystallization; pulse-pressure; diffusion bonding; diffusion coefficient

Evaluation of transverse residual stress in twin wire welded plates by ultrasonic method LU Hao¹, LIU Xuesong¹, YANG Jianguo¹, ZHANG Shiping², FANG Hongyuan¹ (1. State Key Laboratory of Advanced Welding Production Technology, Harbin Institute of Technology, Harbin 150001, China; 2. School of Electrical Engineering and Automation, Harbin Institute of Technology, Harbin 150001, China). p30–32

Abstract Based on the acoustical theory and the simplified acoustoelastic equation for Lcr wave, ultrasonic stress measurement installation was established which consisted of a special transducer and an oscillograph with special higher digitizer board. The Lcr wave which is sensitive to stress is suitable to measure welding residual stress. Acoustoelastic coefficient of longitudinal critically refracted waves propagating in Q235 steel was obtained by tensile testing machine. The transverse stress of twin wire welded plates was measured by this system. The result fluctuation was discussed. The measurement process is real-time and quick which can be as the base of real-time reliability evaluation system for welded structure.

Key words: ultrasonic; Lcr waves; transverse residual stress

Coordinate control of broken-line welding seam tracking for wheeled robot GAO Yanfeng, ZHANG Hua, MAO Zhiwei, PENG Junfei (Key Laboratory of Robot & Welding Automation of Jiangxi, Nanchang University, Nanchang 330031, China). p33–36

Abstract A coordinate control method was proposed for wheeled welding robot with rotational arc as sensor to track broken-line welding seam. Self-turning fuzzy controller was designed to complete coordinately controlling of cross-slider and wheels, and exactly welding seam tracking was realized by use of the controller. To make the robot's moving direction parallel to the welding seam direction, Sugeno fuzzy logic system was used as a filter to process the robot's orientation errors, which makes the robot move along when tracking lined section of welding seam and turn quickly when tracking covered section of welding seam. The experimental results show that the presented method is valid to track 60° broken-line welding seam and Z shape welding seam.

Key words: welding seam tracking; wheeled robot; fuzzy control

Numerical simulation of welding distortion of blisk on aero-engine by controlling heat input ZHANG Xueqiu¹, YANG Jianguo^{1,2}, LIU Xuesong¹, FANG Hongyuan¹, QU Shen² (1. State Key Laboratory of Advanced Welding Production Technology, Harbin Institute of Technology, Harbin 150001, China; 2. Shenyang Liming Aero-Engine Group Corporation, Shenyang 110043, China). p37–40

Abstract Welding distortion of blisk on aero-engines manu-